Characterization of the light absorbing properties, chromophores composition and sources of brown carbon aerosol in Xi'an, Northwest China

Wei Yuan[1,2], Ru-Jin Huang[1,3], Lu Yang[1], Jie Guo[1], Ziyi Chen[4], Jing Duan[1,2], Meng Wang[1,2], Ting Wang[1,2], Haiyan Ni[1], Yongming Han[1], Yongjie Li[5], Qi Chen[6], Yang Chen[7], Thorsten Hoffmann[8], Colin O'Dowd[9]

[1]State Key Laboratory of Loess and Quaternary Geology, Center for Excellence in Quaternary Science and Global Change, Chinese Academy of Sciences, and Key Laboratory of Aerosol Chemistry & Physics, Institute of Earth Environment, Chinese Academy of Sciences, Xi'an 710061, China

[2]University of Chinese Academy of Sciences, Beijing 100049, China

[3]Institute of Global Environmental Change, Xi'an Jiaotong University, Xi'an 710049, China

[4]Royal School of Mines, South Kensington Campus, Imperial College London, Exhibition Road, London SW7 3RW, United Kingdom

[5]Department of Civil and Environmental Engineering, Faculty of Science and Technology, University of Macau, Taipa, Macau 999078, China

[6]State Key Joint Laboratory of Environmental Simulation and Pollution Control, College of Environmental Sciences and Engineering, Peking University, Beijing 100871, China

[7]Chongqing Institute of Green and Intelligent Technology, Chinese Academy of Sciences, Chongqing 400714, China

[8]Institute of Inorganic and Analytical Chemistry, Johannes Gutenberg University Mainz, Duesbergweg 10−14, Mainz 55128, Germany

[9]School of Physics and Centre for Climate and Air Pollution Studies, Ryan Institute, National University of Ireland Galway, University Road, Galway H91CF50, Ireland

Correspondence to: Ru-Jin Huang (rujin.huang@ieecas.cn)

Abstract

The impact of brown carbon aerosol (BrC) on the Earth's radiative forcing balance has

been widely recognized but remains uncertain, mainly because the relationships among BrC sources, chromophores, and optical properties of aerosol are poorly understood. In this work, the light absorption properties and chromophore composition of BrC were investigated for samples collected in Xi'an, Northwest China from 2015 to 2016. Both absorption Ångström exponent and mass absorption efficiency show distinct seasonal differences, which could be attributed to the differences in sources and chromophore composition of BrC. Three groups of light-absorbing organics were found to be important BrC chromophores, including those show multiple absorption peaks at wavelength > 350 nm (12 polycyclic aromatic hydrocarbons and their derivatives) and those show single absorption peak at wavelength < 350 nm (10 nitrophenols and nitrosalicylic acids and 3 methoxyphenols). These measured BrC chromophores show distinct seasonal differences and contribute on average about 1.1% and 3.3% of light absorption of methanol-soluble BrC at 365 nm in summer and winter, respectively, about 7 and 5 times higher than the corresponding carbon mass fractions in total organic carbon. The sources of BrC were resolved by positive matrix factorization (PMF) using these chromophores instead of commonly used non-light absorbing organic markers as model inputs. Our results show that in spring vehicular emissions and secondary formation are major sources of BrC (~70%), in fall coal combustion and vehicular emissions are major sources (~70%), in winter biomass burning and coal combustion become major sources (~80%), while in summer secondary BrC dominates (~60%).

1 Introduction

Brown carbon (BrC) is an important component of atmospheric aerosol particles and has significant effects on radiative forcing and climate (Feng et al., 2013; Laskin et al., 2015; Zhang et al., 2017a). BrC can efficiently absorb solar radiation and reduce the photolysis rates of atmospheric radicals (Jacobsan, 1999; Li et al., 2011; Mok et al., 2016), which ultimately influences the atmospheric photochemistry process, the formation of secondary organic aerosol (SOA), and therefore the regional air quality (Mohr et al., 2013; Laskin et al., 2015; Moise et al., 2015). In addition, some components in BrC, such as nitrated aromatic compounds (NACs) (Teich et al., 2017; Wang et al., 2018) and polycyclic aromatic hydrocarbons (PAHs) (Samburova et al., 2016; Huang et al., 2018), have adverse effects on human health (Bandowe

et al., 2014; Shen et al., 2018). The significant effects of BrC on environment, climate, air quality and living things call for more studies to understand its chemical characteristics, sources and the links with optical properties.

Investigating the chemical composition of BrC at molecular level is necessary, because even small amounts of compounds can have a significant effect on the light absorption properties of BrC and profound atmospheric implication (Mohr et al., 2013; Zhang et al., 2013; Teich et al., 2017; Huang et al., 2018). A number of studies have investigated the BrC composition at molecular level (Mohr et al., 2013; Zhang et al., 2013; Chow et al., 2015; Samburova et al., 2016; Lin et al., 2016, 2017, 2018; Teich et al., 2017; Huang et al., 2018; Lu et al., 2019). For example, Zhang et al. (2013) measured 8 NACs in Los Angeles and found that they contributed about 4% of water-soluble BrC absorption at 365 nm. Huang et al. (2018) measured 18 PAHs and their derivatives in Xi'an and found that they accounted for on average ~1.7% of the overall absorption of methanol-soluble BrC. A state-of-the-art high performance liquid chromatography-photodiode array-high resolution mass spectrometry (HPLC-PDA-HRMS) was applied to investigate the elemental composition of BrC chromophores in biomass burning aerosol (Lin et al., 2016, 2017, 2018). Despite these efforts, the molecular composition of atmospheric BrC still remains largely unknown due to its complexity in emission sources and formation processes.

Field observations and laboratory studies show that BrC has various sources, including primary emissions such as combustion and secondary formation from various atmospheric processes (Laskin et al., 2015). Biomass burning, including forest fires and burning of crop residues, is considered as the main source of BrC (Teich et al., 2017; Lin et al., 2017). Coal burning and vehicle emissions are also important primary sources of BrC (Yan et al., 2017; Xie et al., 2017; Sun et al., 2017; Li et al., 2019; Song et al., 2019). Secondary BrC is produced through multiple-phase reactions occurring in or between gas phase, particle phase, and cloud droplets. For example, nitrification of aromatic compounds (Harrison et al., 2005; Lu et al., 2011), oligomers of acid-catalyzed condensation of hydroxyl aldehyde (De Haan et al., 2009; Shapiro et al., 2009), and reaction of ammonia (NH_3) or amino acids with carbonyls (De Haan et al., 2011; Nguyen et al., 2013; Flores et al., 2014) can all produce BrC. Condensed phase

reactions and aqueous-phase reactions have also been found to be important formation pathways for secondary BrC in ambient air (Gilardoni et al., 2016). In addition, atmospheric aging processes can lead to either enhancement or bleaching of the BrC absorption (Lambe et al., 2013; Lee et al., 2014; Zhong and Jang, 2014), further challenging the characterization of BrC.

As the starting point of the Silk Road, Xi'an is an important inland city in northwestern China experiencing severe particulate air pollution, especially during heating period with enhanced coal combustion and biomass burning activities (Wang et al., 2016; Ni et al., 2018). In this study, we performed spectroscopic measurement and chemical analysis of $PM_{2.5}$ filter samples in Xi'an to investigate: 1) seasonal variations in the light absorption properties and chromophore composition of BrC, and their relationships; 2) sources of BrC in different seasons based on positive matrix factorization (PMF) model with light-absorbing organic markers as input species.

2 Experimental

2.1 Aerosol sampling

A total of 112 daily ambient $PM_{2.5}$ filter samples were collected on pre-baked (780 °C, 3 h) quartz-fiber filters (20.3 × 25.4 cm, Whatman, QM-A, Clifton, NJ, USA) in November-December 2015, April-May, July, October-November 2016, representing winter, spring, summer and fall, respectively. Filter samples were collected using a Hi-Vol $PM_{2.5}$ air sampler (Tisch, Cleveland, OH) at a flow rate of 1.05 m^3 min^{-1} on the roof (~10 m above ground level, 34.22°N, 109.01°E) of the Institute of Earth Environment, Chinese Academy of Sciences, which was surrounded by residential areas without large industrial activities. After collection, the filter samples were wrapped in baked aluminum foils and stored in a freezer (-20 °C) until further analysis.

2.2 Light absorption measurement

One punch of loaded filter (0.526 cm^2) was taken from each sample and sonicated for 30 minutes in 10 mL of ultrapure water (> 18.2 MΩ · cm) or methanol (HPLC grade, J. T. Baker, Phillipsburg, NJ, USA). The extracts were then filtered with a 0.45 μm PTFE pore syringe filter

to remove insoluble materials. The light absorption spectra of water-soluble and methanol-soluble BrC were measured with an UV-Vis spectrophotometer (300-700 nm) equipped with a liquid waveguide capillary cell (LWCC-3100, World Precision Instrument, Sarasota, FL, USA) following the method by Hecobian et al. (2010). The measured absorption data can be converted to the absorption coefficient Abs_λ ($M\ m^{-1}$) by equation (1):

$$Abs_\lambda = (A_\lambda - A_{700})\frac{V_l}{V_a \times L} \times \ln(10) \quad (1)$$

where A_{700} is the absorption at 700 nm, serving as a reference to account for baseline drift, V_l is the volume of water or methanol that the filter was extracted into, V_a is the volume of sampled air, L is the optical path length (0.94 m). A factor of ln(10) is used to convert the log base-10 (recorded by UV-Vis spectrophotometer) to natural logarithm to provide base-e absorption coefficient. The absorption coefficient of water-soluble or methanol-soluble organics at 365 nm (Abs_{365}) is used to represent water-soluble or methanol-soluble BrC absorption, respectively.

The mass absorption efficiency (MAE: $m^2\ gC^{-1}$) of BrC in the extracts can be calculated as:

$$MAE_\lambda = \frac{Abs_\lambda}{M} \quad (2)$$

where M ($\mu gC\ m^{-3}$) is the concentration of water-soluble organic carbon (WSOC) for water extracts or methanol-soluble organic carbon (MSOC) for methanol extracts. Note that organic carbon (OC) is often used to replace MSOC because direct measurement of MSOC is technically difficult and many studies have shown that most of OC (~ 90%) can be extracted by methanol (Chen and Bond, 2010; Cheng et al., 2016; Xie et al., 2019).

The wavelength-dependent light absorption of chromophores in solution, termed as absorption Ångström exponent (AAE), can be described as:

$$Abs_\lambda = K \cdot \lambda^{-AAE} \quad (3)$$

where K is a constant related to the concentration of chromophores and AAE is calculated by linear regression of $\log Abs_\lambda$ versus $\log \lambda$ in the wavelength range of 300-410 nm.

2.3 Chemical analysis

OC was measured with a thermal/optical carbon analyzer (DRI, model 2001) following the IMPROVE-A protocol (Chow et al., 2011). WSOC was measured with a TOC/TN analyzer

(TOC−L, Shimadzu, Japan) (Ho et al., 2015).

Organic compounds listed in Table S1 were analyzed with a gas chromatograph-mass spectrometer (GC-MS, Agilent Technologies, Santa Clara, CA, USA). Prior to the GC-MS analysis, the silylation derivatization was conducted using a routine method (e.g., Wang et al., 2016; Al-Naiema and stone, 2017). Briefly, a quarter of 47 mm filter sample was ultrasonically extracted with 2 mL of methanol for 15 minutes and repeated three times. The extracts were filtered with a 0.45 μm PTFE syringe filter and then evaporated with a rotary evaporator to ~1 mL and dried with a gentle stream of nitrogen. Then, 50 μL of N,O-bis(trimethylsilyl)trifluoroacetamide (BSTFA-TMCS; Fluka Analytical 99%) and 10 μL of pyridine were added. The mixture was heated for 3 h at 70 ºC for silylation. After reaction, 140 μL of n-hexane were added to dilute the derivatives. Finally, 2 μL aliquot of the derivatized extracts were introduced into the GC-MS, which was equipped with a DB-5MS column (Agilent Technologies, Santa Clara, CA, USA), electron impact (EI) ionization source (70 eV), and a GC inlet of 280 ºC. The GC oven temperature was held at 50 ºC for 2 min, ramped to 120 ºC at a rate of 15 ºC min^{-1}, and finally reached 300 ºC at a rate of 5 ºC min^{-1} (held for 16 min). Note that the derivatization for NACs was conducted at 70 ºC for 3 h which is slightly different from the protocol used in Al-Naiema and stone (2017), because symmetrical peak shapes and high intensities for NACs can also be obtained under this condition in our study (see Fig. S1). In our study, 4-nitrophenol-2,3,5,6-d4 was used as an internal standard to correct for potential loss for NACs quantification (Chow et al., 2015). For the quantification of other organic compounds, an external standard method was used through daily calibration with working standard solutions. Also, for every 10 samples, a procedural blank and a spiked sample (i.e., ambient sample spiked with known amounts of standards) were measured to check the interferences and recoveries. The measured recoveries are 80-102% and the uncertainties (RSDs) are < 10% for measured organic compounds.

2.4 Source apportionment of BrC

Source apportionment of methanol-soluble BrC was performed using positive matrix factorization (PMF) as implemented by the multilinear engine (ME-2; Paatero, 1997) via the Source Finder (SoFi) interface written in Igor Wavemetrics (Canonaco et al., 2013). $Abs_{365,MSOC}$

and those light-absorbing species including fluoranthene (FLU), pyrene (PYR), chrysene (CHR), benzo(a)anthracene (BaA), benzo(a)pyrene (BaP), benzo(b)fluoranthene (BbF), benzo(k)fluoranthene (BkF), indeno[1,2,3-cd]pyrene (IcdP), benzo(ghi)perylene (BghiP), 9,10-anthracenequinone (9,10AQ), benzanthrone (BEN), benzo[b]fluoren-11-one (BbF11O), vanillic acid, vanillin and syringyl acetone were used as model inputs, together with some commonly used markers, i.e., phthalic acid, hopanes (17α(H),21β(H)-30-norhopane, 17α(H),21β(H)-hopane, 17α(H),21β(H)-(22S)-homohopane, 17α(H),21β(H)-(22R)-homohopane, referred to as HP1-HP4, respectively), picene, and levoglucosan. The input data include species concentrations and uncertainties. The method detection limits (MDLs), calculated as three times of the standard deviation of the blank filters, were used to estimate species-specific uncertainties, following Liu et al. (2017). Furthermore, for a clear separation of sources profiles, the contribution of corresponding markers was set to 0 in the sources unrelated to the markers (see Table S2). This source apportionment protocol is very similar to our previous study (Huang et al., 2014).

3 Results and discussion

3.1 Light absorption properties of water- and methanol-soluble BrC

Fig. 1 shows the temporal profiles of Abs_{365} of water- and methanol-soluble BrC, together with the concentrations of WSOC and OC (representing MSOC). They all show similar seasonal variations with the highest average in winter, followed by fall, spring and summer (see Table S3). WSOC contributed annually 54.4 ± 16.2% of the OC mass, with the highest contribution in summer (66.1 ± 15.5%) and the lowest contribution in winter (45.1 ± 10.2%). The higher WSOC fraction in OC during summer is largely contributed by SOA and to some extent by biomass burning emissions because both SOA and biomass burning OA consist of high fraction of WSOC (Ram et al., 2012; Yan et al., 2015; Daellenbach et al., 2016). The lower WSOC fractions in OC during winter could be attributed to enhanced emissions from coal combustion which produce a large fraction of water-insoluble organics (Daellenbach et al., 2016; Yan et al., 2017). $Abs_{365,MSOC}$ is approximately 2 times (range 1.7-2.3) higher than $Abs_{365,WSOC}$, which is similar to the results measured in Beijing (Cheng et al., 2016),

southeastern Tibetan Plateau (Zhu et al., 2018), Gwangju, Korea (Park et al., 2018) and the Research Triangle Park, USA (Xie et al., 2019), indicating that the optical properties of BrC could be largely underestimated when using water as the extracting solvent as non-polar fraction of BrC is also important to light absorption of BrC (Sengupta et al., 2018). In Fig. S2 we summarized those previously reported $Abs_{365,WSOC}$ (as $Abs_{365,MSOC}$ was not commonly measured in many previous studies) values at different sites in Asian urban and remote areas and the US. $Abs_{365,WSOC}$ is significantly higher in most Asian urban regions than in the Asian remote sites and the US, and show clear seasonal variations. The high light absorption of BrC in Asian urban regions, especially during winter, may have important effects on regional climate and radiation forcing (Park et al., 2010; Laskin et al., 2015). As discussed in Feng et al. (2013), the average global climate forcing of BrC was estimated to be 0.04-0.11 W m^{-2} and above 0.25 W m^{-2} in urban sites of south and east Asia regions, which is about 25% of the radiative forcing of black carbon (BC, 1.07 W m^{-2}). Thus, to further understand the influence of BrC on regional radiation forcing, it is essential to identify and quantify the sources of BrC in Asia.

The seasonal averages of AAE of water-soluble BrC were between 5.32 and 6.15 without clear seasonal trend (see Table S3). The seasonal averages of AAE of methanol-soluble BrC were relatively lower than those of water-soluble BrC, ranging from 4.45 to 5.18 which is similar to the results in Los Angeles Basin (Zhang et al., 2013) and Gwangju, Korea (Park et al., 2018). This is because methanol can extract more compounds with high conjugation degree and strong light-absorbing capability (e.g., PAHs) at longer wavelength (> 350 nm) (Samburova et al., 2016). The AAE values of water-soluble BrC (as AAE of methanol-soluble BrC was not commonly measured in many previous studies) in urban, rural and remote regions show a large difference (see Fig. 2a), typically with much lower AAE values in urban regions than those in rural and remote regions, indicating the difference in sources and chemical composition of chromophores. The urban regions are mainly affected by anthropogenic emissions. Therefore, urban BrC may contain a large amount of aromatic chromophores with high conjugation degree, which absorb light at a longer wavelength and have lower AAE values (Lambe et al., 2013; Wang et al., 2018).

The average MAE_{365} values of water- and methanol-soluble BrC show large seasonal

variations, with highest values in winter (1.85 and 1.50 $m^2\ gC^{-1}$, respectively), followed by fall (1.18 and 1.52 $m^2\ gC^{-1}$), spring (1.01 and 0.79 $m^2\ gC^{-1}$), and summer (0.91 and 1.21 $m^2\ gC^{-1}$). Such large seasonal differences indicate seasonal difference in BrC sources. For example, contributions from coal burning and biomass burning were much larger in winter than in other seasons due to large residential heating activities (also see Section 3.3 for more details). Compared to previous studies (Fig. 2b), the average values of $MAE_{365,WSOC}$ are obviously higher in urban sites than in rural and remote sites that are less influenced by anthropogenic activities. The higher $MAE_{365,WSOC}$ values in urban regions is likely associated with enhanced anthropogenic emissions from e.g., coal combustion and biomass burning, and the lower $MAE_{365,WSOC}$ values in rural and remote regions could be attributed to biogenic sources or aged secondary BrC (Lei et al., 2018; Xie et al., 2019).

3.2 Chemical characterization of the BrC chromophores

Given the complexity in emission sources and formation processes, the molecular composition of atmospheric BrC remains largely unknown. PAHs, NACs and MOPs have recently been found as major chromophores in biomass burning-derived BrC (Lin et al., 2016, 2017, 2018). However, these compounds can also be directly emitted by coal combustion and motor vehicle or formed by secondary reactions (Harrison et al., 2005; Iinuma et al., 2010; Liu et al., 2017; Wang et al., 2018; Lu et al., 2019), making source attribution of atmospheric BrC more challenging. To obtain the exact molecular composition of BrC chromophores and understand the influence of a specific chromophore on BrC optical property, we measured the light absorption characteristics of available chromophore standards including 12 PAHs, 10 NACs and 3 MOPs, and quantified their concentrations in $PM_{2.5}$ samples with GC-MS. The light absorption contribution of individual chromophores to that of methanol-soluble BrC in the wavelength range of 300-500 nm was estimated according to its concentration and mass absorption efficiency (see Supplementary). Fig. 3 shows the contribution of carbon content in identified BrC chromophores to the total OC mass. They all show obvious seasonal variations with the highest values in winter and lowest in summer. The seasonal difference can be up to a factor of 5-6. The contribution of PAHs ranged from 0.12% in summer to 0.47% in winter, NACs from 0.02% in summer to 0.13% in winter, and MOPs from 0.01% in summer to 0.06%

in winter. It should be noted that NACs are dominated by 4-nitrophenol and 4-nitrocatechol in spring, fall and winter, but by 4-nitrophenol and 5-nitrosalicylic acid in summer. The difference is likely due to enhanced summertime formation of 5-nitrosalicylic acid, which is more oxidized than other nitrated phenols measured in this study (Wang et al., 2018).

The seasonally averaged contributions of PAHs, NACs, MOPs and total measured chromophores to light absorption of methanol-soluble BrC between 300 to 500 nm are shown in Fig. 4. They show large seasonal variations and wavelength dependence. Specifically, PAHs made the largest contribution to BrC light absorption in fall, followed by winter, spring and summer, and show two large absorption peaks at about 365 nm and 380 nm, which are mainly associated with the absorption of BaP, BghiP, IcdP, FLU, BkF and BaA (see Fig. S3). Compared to PAHs, NACs show the largest contribution in winter, followed by fall, spring and summer, and exhibit only one absorption peak at about 320 nm in spring and summer and at about 330 nm in fall and winter. The red shift in the absorption peak could be attributed to the increase of contributions from 4-nitrocatechol, 4-methyl-5nitrocatechol and 3-methyl-5-nitrocatechol which have absorption peak at about 330-350 nm (see Fig. S3). Different from PAHs and NACs, MOPs contribute the most in winter, followed by spring, fall and summer, and only show one absorption peak at about 310 nm. The difference in light absorption contributions of different chromophores in different seasons reflects the difference in sources, emission strength and atmospheric formation processes.

The total contributions of PAHs, NACs and MOPs to the light absorption of methanol-soluble BrC ranged from 0.47% (summer) to 1.56% (winter) at the wavelength of 300-500 nm and ranged from 1.05% (summer) to 3.26% (winter) at the wavelength of 365 nm (see Table 1). The average contribution of PAHs to the BrC light absorption at 365 nm was 0.97% in summer (the lowest) and 2.69% in fall (the highest), the contribution of NACs was 0.09% in summer and 0.82% in winter, and the contribution of MOPs was 0.006% in summer and 0.024% in winter. The low contributions of these measured chromophores to the light absorption of methanol-soluble BrC are consistent with previous studies. For example, Huang et al. (2018) measured 18 PAHs and their derivatives, which on average contributed ~1.7% of the overall absorption of methanol-soluble BrC in Xi'an. Mohr et al. (2013) estimated the contribution of

five NACs to particulate BrC light absorption at 370 nm to be ~4% in Detling, UK. Zhang et al. (2013) measured eight NACs, which accounted for ~4% of water-soluble BrC absorption at 365 nm in Los Angeles. Teich et al. (2017) determined eight NACs during six campaigns at five locations in summer and winter, and founded that the mean contribution of NACs to water-soluble BrC absorption at 370 nm ranged from 0.10% to 1.25% under acidic conditions and from 0.13% to 3.71% under alkaline conditions. Slightly different from these previous studies, we investigated the contributions of three groups of chromophores with different light-absorbing properties to the light absorption of BrC, and provided further understanding in the relationships between optical properties and chemical composition of BrC in the atmosphere. For example, vanillin, which has negligible contribution to BrC light absorption at 365 nm, can produce secondary BrC through oxidation and thus enhance the light absorption by a factor of 5-7 (Li et al., 2014; Smith et al., 2016). The contribution of PAHs to the light absorption of methanol-soluble BrC at 365 nm was 5-13 times that of their mass fraction of carbon in OC, 6-9 times for NACs, and 0.4-0.7 times for MOPs (4-8 times at 310 nm for MOPs). These results further demonstrate that even a small amount of chromophores can have a disproportionately high impact on the light absorption properties of BrC, and that the light absorption of BrC is likely determined by a number of chromophores with strong light absorption ability (Kampf et al., 2012; Teich et al., 2017). Of note, a large fraction of BrC chromophores are still not identified so far, and more studies are therefore necessary to better understand the BrC chemistry. Based on laboratory and ambient studies, imidazoles (Kampf et al., 2012; Teich et al., 2016), quinones (Lee et al., 2014; Pillar et al., 2017), nitrogenous PAHs (Lin et al., 2016; Lin et al., 2018), polyphenols (Lin et al., 2016; Pillar et al., 2017) and oligomers with higher conjugation (Lin et al., 2014; Lavi et al., 2017) could be included in future studies.

3.3 Sources of BrC

Two approaches have been used to quantify the sources of BrC, including multiple linear regression and receptor models such as PMF. For example, Washenfelder et al. (2015) utilized multiple linear regression to determine the contribution of individual OA factors resolved by PMF to OA light absorption in the southeastern America. Moschos et al. (2018) combined the time series of PMF-resolved OA factors with the time series of light absorption of water-soluble

OA extract as model inputs to quantify the sources of BrC in Magadino and Zurich, Switzerland. Xie et al. (2019) quantified the sources of BrC in southeastern America using Abs_{365}, elemental carbon (EC), OC, WSOC, isoprene sulfate ester, monoterpene sulfate ester, levoglucosan and isoprene SOA tracers as PMF model inputs. However, it should be noted that previous studies mainly rely on the correlation between measured light absorption and organic tracers that do not contain a BrC chromophore, and therefore may lead to bias in BrC source apportionment. To better constrain the sources of BrC (i.e., contribution to $Abs_{365,MSOC}$), we used BrC chromophores as PMF model inputs. The inputs include vanillic acid, vanillin, and syringyl acetone for BrC from biomass burning, and FLU, PYR, CHR, BaA, BaP, BbF, BkF, IcdP, BghiP, for BrC from incomplete combustion and other light absorbing chromophores 9,10AQ, BEN, and BbF11O. In addition, we included commonly used markers levoglucosan for biomass burning, phthalic acid for secondary BrC, hopanes for vehicle emission and picene for coal burning in the model inputs.

Four factors were resolved, including vehicle emission, coal burning, biomass burning and secondary formation. The uncertainties for PMF analysis are < 10% for secondary formation and biomass burning, < 15% for vehicle emission and coal burning. The profile of each factor is shown in Fig. S4. The first factor is characterized by a high contribution of phthalic acid, a tracer of secondary formation of OA. The second factor is dominated by hopanes, mainly from vehicular emissions. The third factor is characterized by high contributions of PI, BaP, BbF, BkF, IcdP, BghiP, mainly from coal combustion emissions, while the fourth factor has high contributions of levoglucosan, vanillic acid, vanillin, syringyl acetone from biomass burning emissions. The seasonal difference in relative contribution of each factor to BrC light absorption is shown in Fig. 5. In spring, vehicular emissions (34%) and secondary formation (37%) were the main contributors to BrC and coal combustion also had a relatively large contribution (29%). In summer, secondary formation constituted the largest fraction (~60%), mainly due to enhanced photochemical formation of secondary BrC. In fall, vehicular emissions (38%), coal combustion (29%) and biomass burning (22%) all had significant contributions to BrC. In winter, coal combustion (44%) and biomass burning (36%) were the main contributors, due to emissions from residential biomass burning (wood and crop residues) and coal combustion for

heating. In terms of absolute contributions to absorption of MSOC at 365 nm (see Table S4), secondary formation contributed 1.75, 2.55, 1.70, 6.20 M m^{-1} in spring, summer, fall and winter, respectively. The high contribution in winter can be attributed to abundant precursors (volatile organic compounds) co-emitted with other primary sources (especially coal burning and biomass burning), while the high contribution in summer might be due to strong photochemical activity. For spring and fall, the absolute contributions from secondary formation were very similar, indicating moderate precursor emission and moderate photochemical activity. Also it should be noted that the absolute contributions of vehicle emission to absorption of MSOC at 365 nm were still higher in spring and fall than those in summer and winter, yet these differences by a factor of 2-9 are still less pronounced than the differences (spring/fall vs. winter) for other primary emissions (> 40 times for coal burning and > 25 times for biomass burning). In particular, the high vehicle contribution in fall might be affected by high relative humidity in fall (83% in fall vs. 61-69% in other seasons, on average) resulting in high vehicular $PM_{2.5}$ emissions (Chio et al., 2010). Such large seasonal difference in emission sources and atmospheric processes of BrC indicates that more studies are required to better understand the relationship between chemical composition, formation processes, and light absorption properties of BrC.

4 Conclusion

The light absorption properties of water- and methanol-soluble BrC in different seasons were investigated in Xi'an. The light absorption coefficient of methanol-soluble BrC was approximately 2 times higher than that of water-soluble BrC at 365 nm, and had an average MAE_{365} value of 1.27 ± 0.46 m^2 gC^{-1}. The average MAE_{365} value of water-soluble BrC was 1.19 $\pm$ 0.51 m^2 gC^{-1}, which is comparable to those in previous studies at urban sites but higher than those in rural and remote areas. The seasonally averaged AAE values of water-soluble BrC ranged from 5.32 to 6.15, which are higher than those of methanol-soluble BrC (between 4.45 and 5.18). In combination with previous studies, we found that AAE values of water-soluble BrC were much lower in urban regions than those in rural and remote regions. The difference of optical properties of BrC in different regions could be attributed to the difference in sources and chemical composition of BrC chromophores. The contributions of 12 PAHs, 10 NACs and

3 MOPs to the light absorption of methanol-soluble BrC were determined and showed large seasonal variations. Specifically, the total contribution to methanol-soluble BrC light absorption at 365 nm ranged from 1.1% to 3.3%, which is 5-7 times higher than their carbon mass fractions in total OC. This result indicates that the light absorption of BrC is likely determined by an amount of chromophores with strong light absorption ability. Four major sources of methanol-soluble BrC were identified, including secondary formation, vehicle emission, coal combustion and biomass burning. On average, secondary formation and vehicular emission were the main contributors of BrC in spring (~70%). Vehicular emission (38%), coal burning (29%) and biomass burning (22%) all contributed significantly to BrC in fall. Coal combustion and biomass burning were the major contributors in winter (~80%), and secondary formation was the predominant source in summer (~60%). The large variations of BrC sources in different seasons suggest that more studies are needed to understand the seasonal difference in chemical composition, formation processes, and light absorption properties of BrC, as well as their relationships.

5 Abbreviations of organics

PAHs (Polycyclic Aromatic Hydrocarbons)

BaA	Benzo(a)anthracene
BaP	Benzo(a)pyrene
BbF	Benzo(b)fluoranthene
BbF11O	Benzo[b]fluoren-11-One
BEN	Benzanthrone
BghiP	Benzo(ghi)perylene
BkF	Benzo(k)fluoranthene
CHR	Chrysene
FLU	Fluoranthene
IcdP	Indeno[1,2,3-cd]pyrene
PYR	Pyrene
9,10AQ	9,10-Anthracenequinone

NACs (Nitrated Aromatic Compounds)

2M4NP	2-Methyl-4-Nitrophenol
2,6DM4NP	2,6-Dimethyl-4-Nitropheol
3M4NP	3-Methyl-4-Nitrophenol
3M5NC	3-Methyl-5-Nitrocatechol
3NSA	3-Nitrosalicylic Acid
4M5NC	4-Methyl-5-Nitrocatechol
4NC	4-Nitrocatechol
4NP	4-Nitrophenol
4N1N	4-Nitro-1-Naphthol
5NSA	5-Nitrosalicylic Acid

MOP (Methoxyphenols)

SyA	Syringyl Acetone
VaA	Vanillic Acid
VAN	Vanillin

Hopanes

HP1	17α(H),21β(H)-30-Norhopane
HP2	17α(H),21β(H)-Hopane
HP3	17α(H),21β(H)-(22S)-Homohopane
HP4	17α(H),21β(H)-(22R)-Homohopane

Data availability. Raw data used in this study are archived at the Institute of Earth Environment, Chinese Academy of Sciences, and are available on request by contacting the corresponding author.

Supplement. The Supplement related to this article is available online at

Author contributions. RJH designed the study. Data analysis was done by WY, LY, and RJH.

WY, LY and RJH interpreted data, prepared the display items and wrote the manuscript. All authors commented on and discussed the manuscript.

Acknowledgements. This work was supported by the National Natural Science Foundation of China (NSFC) under grant no. 41877408, 41925015, and no. 91644219, the Chinese Academy of Sciences (no. ZDBS-LY-DQC001), the Cross Innovative Team fund from the State Key Laboratory of Loess and Quaternary Geology (SKLLQG) (no. SKLLQGTD1801), and the National Key Research and Development Program of China (no. 2017YFC0212701). Yongjie Li acknowledges funding support from the National Natural Science Foundation of China (41675120), the Science and Technology Development Fund, Macau SAR (File no. 016/2017/A1), and the Multi-Year Research grant (No. MYRG2018-00006-FST) from the University of Macau.

References

Al-Naiema, I. M., and Stone, E. A.: Evaluation of anthropogenic secondary organic aerosol tracers from aromatic hydrocarbons, Atmos. Chem. Phys., 17, 2053-2065, doi:10.5194/acp-17-2053-2017, 2017.

Bandowe, B. A. M., Meusel, H., Huang, R-J., Ho, K., Cao, J., Hoffmann, T., and Wilcke, W.: PM2.5-bound oxygenated PAHs, nitro-PAHs and parent-PAHs from the atmosphere of a Chinese megacity: Seasonal variation, sources and cancer risk assessment, Sci. Total Environ., 473-474, 77-87, 2014.

Bosch, C., Andersson, A., Kirillova, E. N., Budhavant, K., Tiwari, S., Praveen, P. S., Russell, L. M., Beres, N. D., Ramanathan, V., and Gustafsson, Ö.: Source-diagnostic dual-isotope composition and optical properties of water-soluble organic carbon and elemental carbon in the South Asian outflow intercepted over the Indian Ocean, J. Geophys. Res. Atmos., 119, 11743-11759, doi:10.1002/2014JD022127, 2014.

Chen, Y., and Bond, T. C.: Light absorption by organic carbon from wood combustion, Atmos. Chem. Phys., 10, 1773-1787, doi:10.5194/acp-10-1773-2010, 2010.

Chen, Y., Ge, X., Chen, H., Xie, X., Chen, Y., Wang, J., Ye, Z., Bao, M., Zhang, Y., and Chen, M.: Seasonal light absorption properties of water-soluble brown carbon in atmospheric

fine particles in Nanjing, China, Atmos. Environ., 187, 230-240, doi:10.1016/j.atmosenv.2018.06.002, 2018.

Cheng, Y., He, K. B., Du, Z. Y., Engling, G., Liu, J. M., Ma, Y. L., Zheng, M., and Weber, R. J.: The characteristics of brown carbon aerosol during winter in Beijing, Atmos. Environ., 127, 355-364, doi:10.1016/j.atmosenv.2015.12.035, 2016.

Choi, D., Beardsley, M., Brzezinski, D., Koupal, J., and Warila, J.: MOVES sensitivity analysis: the impacts of temperature and humidity on emissions, [online] Available from: https://www3.epa.gov/ttnchie1/conference/ei19/session6/choi.pdf, 2010.

Chow, J. C., Watson, J. G., Robles, J., Wang, X. L., Antony Chen, L. W., Trimble, D. L., Kohl, S. D., Tropp, R. J., and Fung, K. K.: Quality assurance and quality control for thermal/optical analysis of aerosol samples for organic and elemental carbon, Anal. Bioanal. Chem., 401, 3141- 3152, doi:10.1007/s00216-011-5103-3, 2011.

Chow, K. S., Huang, X. H. H., and Yu, J. Z.: Quantification of nitroaromatic compounds in atmospheric fine particulate matter in Hong Kong over 3 years: field measurement evidence for secondary formation derived from biomass burning emissions, Environ. Chem., 13, 665-673, doi:10.1071/EN15174, 2015.

Canonaco, F., Crippa, M., Slowik, J. G., Baltensperger, U., and Prévôt, A. S. H.: SoFi, an IGOR based interface for the efficient use of the generalized multilinear engine (ME-2) for the source apportionment: ME-2 application to aerosol mass spectrometer data, Atmos. Meas. Tech., 6, 3649-3661, doi:10.5194/amt-6-3649-2013, 2013.

Daellenbach, K. R., Bozzetti, C., Krepelova, A. K., Canonaco, F., Wolf, R., Zotter, P., Fermo, P., Crippa, M., Slowik, J. G., Sosedova, Y., Zhang, Y., Huang, R. J., Poulain, L., Szidat, S., Baltensperger, U., El Haddad, I., and Prevot, A. S. H.: Characterization and source apportionment of organic aerosol using offline aerosol mass spectrometry, Atmos. Meas. Tech., 9, 23-39, doi:10.5194/amt-9-23-2016, 2016.

De Haan, D. O., Corrigan, A. L., Smith, K. W., Stroik, D. R., Turley, J. J., Lee, F. E., Tolbert, M. A., Jimenez, J. L., Cordova, K. E., and Ferrell, G. R.: Secondary organic aerosol-forming reactions of glyoxal with amino acids, Environ. Sci. Technol., 43, 2818-2824, doi:10.1021/es803534f, 2009.

De Haan, D. O., Hawkins, L. N., Kononenko, J. A., Turley, J. J., Corrigan, A. L., Tolbert, M. A., and Jimenez, J. L.: Formation of nitrogen-containing oligomers by methylglyoxal and amines in simulated evaporating cloud droplets, Environ. Sci. Technol., 45, 984-991, doi:10.1021/es102933x, 2011.

Feng, Y., Ramanathan, V., and Kotamarthi, V. R.: Brown carbon: A significant atmospheric absorber of solar radiation?, Atmos. Chem. Phys., 13, 8607-8621, doi:10.5194/acp-13-8607-2013, 2013.

Flores, J. M., Washenfelder, R. A., Adler, G., Lee, H. J., Segev, L., Laskin, J., Laskin, A., Nizkorodov, S. A., Brown, S. S., and Rudich, Y.: Complex refractive indices in the near-ultraviolet spectral region of biogenic secondary organic aerosol aged with ammonia, Phys. Chem. Chem. Phys., 16, 10629-10642, doi:10.1039/c4cp01009d, 2014.

Gilardoni, S., Massoli, P., Paglione, M., Giulianelli, L., Carbone, C., Rinaldi, M., Decesari, S., Sandrini, S., Costabile, F., Gobbi, G. P., Pietrogrande, M. C., Visentin, M., Scotto, F., Fuzzi, S., and Facchini, M. C.: Direct observation of aqueous secondary organic aerosol from biomass-burning emissions, Proc. Natl. Acad. Sci., 113, 10013-10018, doi:10.1073/pnas.1602212113, 2016.

Harrison, M. A. J., Barra, S., Borghesi, D., Vione, D., Arsene, C., and Olariu, R. I.: Nitrated phenols in the atmosphere: a review, Atmos. Environ., 39, 231-248, doi:10.1016/j.atmosenv.2004.09.044, 2005.

Hecobian, A., Zhang, X., Zheng, M., Frank, N. H., Edgerton, E. S., and Weber, R. J.: Water-soluble organic aerosol material and the light absorption characteristics of aqueous extracts measured over the Southeastern United States, Atmos. Chem. Phys., 10, 5965-5977, doi:10.5194/acp-10-5965-2010, 2010.

Ho, K. F., Ho, S. S. H., Huang, R. J., Liu, S. X., Cao, J. J., Zhang, T., Chuang, H. C., Chan, C. S., Hu, D., and Tian, L.: Characteristics of water-soluble organic nitrogen in fine particulate matter in the continental area of China, Atmos. Environ., 106, 252-261, doi:10.1016/j.atmosenv.2015.02.010, 2015.

Huang, R. J., Zhang, Y. L., Bozzetti, C., Ho, K. F., Cao, J. J., Han, Y. M., Daellenbach, K. R., Slowik, J. G., Platt, S. M., Canonaco, F., Zotter, P., Wolf, R., Pieber, S. M., Bruns, E. A.,

Crippa, M., Ciarelli, G., Piazzalunga, A., Schwikowski, M., Abbaszade, G., Schnelle-Kreis, J., Zimmermann, R., An, Z. S., Szidat, S., Baltensperger, U., El Haddad, I., and Prévôt, A. S. H.: High secondary aerosol contribution to particulate pollution during haze events in China, Nature, 514, 218-222, 2014.

Huang, R. J., Yang, L., Cao, J., Chen, Y., Chen, Q., Li, Y., Duan, J., Zhu, C., Dai, W., Wang, K., Lin, C., Ni, H., Corbin, J. C., Wu, Y., Zhang, R., Tie, X., Hoffmann, T., O'Dowd, C., and Dusek, U.: Brown carbon aerosol in urban Xi'an, Northwest China: the composition and light absorption properties, Environ. Sci. Technol., 52, 6825-6833, doi:10.1021/acs.est.8b02386, 2018.

Iinuma, Y., Böge, O., Gräfe, R., and Herrmann, H.: Methyl-nitrocatechols: atmospheric tracer compounds for biomass burning secondary organic aerosols, Environ. Sci. Technol., 44, 8453-8459, doi:10.1021/Es102938a, 2010.

Jacobson, M. Z.: Isolating nitrated and aromatic aerosols and nitrated aromatic gases as sources of ultraviolet light absorption, J. Geophys. Res., 104, 3527-3542, doi:10.1029/1998jd100054, 1999.

Kampf, C. J., Jakob, R., and Hoffmann, T.: Identification and characterization of aging products in the glyoxal/ammonium sulfate system - implications for light-absorbing material in atmospheric aerosols, Atmos. Chem. Phys., 12, 6323-6333, doi:10.5194/acp-12-6323-2012, 2012.

Kirillova, E. N., Andersson, A., Han, J., Lee, M., and Gustafsson, Ö.: Sources and light absorption of water-soluble organic carbon aerosols in the outflow from northern China, Atmos. Chem. Phys., 14, 1413-1422, 2014a.

Kirillova, E. N., Andersson, A., Tiwari, S., Srivastava, A. K., Bisht, S. D., and Gustafsson, Ö.: Water-soluble organic carbon aerosols during a full New Delhi winter: Isotope-based source apportionment and optical properties, J. Geophys. Res. Atmos., 119, 3476−3485, 2014b.

Lambe, A. T., Cappa, C. D., Massoli, P., Onasch, T. B., Forestieri, S. D., Martin, A. T., Cummings, M. J., Croasdale, D. R., Brune, W. H., Worsnop, D. R., and Davidovits, P.: Relationship between oxidation level and optical properties of secondary organic aerosol,

Environ. Sci. Technol., 47, 6349-6357, doi:10.1021/es401043j, 2013.

Laskin, A., Laskin, J., and Nizkorodov, S. A.: Chemistry of atmospheric brown carbon, Chem. Rev., 115, 4335-4382, doi:10.1021/cr5006167, 2015.

Lavi, A., Lin, P., Bhaduri, B., Carmieli, R., Laskin, A., and Rudich, Y.: Characterization of Light-Absorbing Oligomers from Reactions of Phenolic Compounds and Fe(III), ACS Earth and Space Chemistry, 1, 637-646, 2017.

Lee, H. J., Aiona, P. K., Laskin, A., Laskin, J., and Nizkorodov, S. A.: Effect of solar radiation on the optical properties and molecular composition of laboratory proxies of atmospheric brown carbon, Environ. Sci. Technol., 48, 10217-10226, 2014.

Lei, Y. L., Shen, Z. X., Wang, Q. Y., Zhang, T., Cao, J. J., Sun, J., Zhang, Q., Wang, L. Q., Xu, H. M., Tian, J., and Wu, J. M.: Optical characteristics and source apportionment of brown carbon in winter $PM_{2.5}$ over Yulin in Northern China, Atmos. Res., 213, 27-33, doi:10.1016/j.atmosres.2018.05.018, 2018.

Li, G., Bei, N., Tie, X., and Molina, L. T.: Aerosol effects on the photochemistry in Mexico City during MCMA-2006/MILAGRO campaign, Atmos. Chem. Phys., 11, 5169-5182, doi:10.5194/acp-11-5169-2011, 2011.

Li, M. J., Fan, X. J., Zhu, M. B., Zou, C. L., Song, J. Z., Wei, S. Y., Jia, W. L., and Peng, P. A.: Abundance and Light Absorption Properties of Brown Carbon Emitted from Residential Coal Combustion in China, Environ. Sci. Technol., 53, 595-603, 2019.

Li, Y. J., Huang, D. D., Cheung, H. Y., Lee, A. K. Y., and Chan, C. K.: Aqueous-phase photochemical oxidation and direct photolysis of vanillin - a model compound of methoxy phenols from biomass burning, Atmos. Chem. Phys., 14, 2871-2885, doi:10.5194/acp-14-2871-2014, 2014.

Lin, Y., Budisulistiorini, S. H., Chu, K., Siejack, R. A., Zhang, H., Riva, M., Zhang, Z., Gold, A., Kautzman, K. E., and Surratt, J. D.: Light-Absorbing Oligomer Formation in Secondary Organic Aerosol from Reactive Uptake of Isoprene Epoxydiols, Environ. Sci. Technol., 48, 12012-12021, doi:10.1021/es503142b, 2014.

Lin, P., Aiona, P. K., Li, Y., Shiraiwa, M., Laskin, J., Nizkorodov, S. A., and Laskin, A.: Molecular characterization of brown carbon in biomass burning aerosol particles, Environ.

Sci. Technol., 50, 11815-11824, doi:10.1021/acs.est.6b03024, 2016.

Lin, P., Bluvshtein, N., Rudich, Y., Nizkorodov, S. A., Laskin, J., and Laskin, A.: Molecular chemistry of atmospheric brown carbon inferred from a nationwide biomass burning event, Environ. Sci. Technol., 51, 11561-11570, doi:10.1021/acs.est.7b02276, 2017.

Lin, P., Fleming, L. T., Nizkorodov, S. A., Laskin, J., and Laskin, A.: Comprehensive Molecular Characterization of Atmospheric Brown Carbon by High Resolution Mass Spectrometry with Electrospray and Atmospheric Pressure Photoionization, Anal. Chem., 90, 12493-12502, doi:10.1021/acs.analchem.8b02177, 2018.

Liu, Y., Yan, C. Q., Ding, X., Wang, X. M., Fu, Q. Y., Zhao, Q. B., Zhang, Y. H., Duan, Y. S., Qiu, X. H., and Zheng, M.: Sources and spatial distribution of particulate polycyclic aromatic hydrocarbons in Shanghai, China, Sci. Total Environ., 584-585, 307-317, doi:10.1016/j.scitotenv.2016.12.134, 2017.

Lu, C., Wang, X., Li, R., Gu, R., Zhang, Y., Li, W., Gao, R., Chen, B., Xue, L., and Wang, W.: Emissions of fine particulate nitrated phenols from residential coal combustion in China, Atmos. Environ., 203, 10-17, doi:10.1016/j.atmosenv.2019.01.047, 2019.

Lu, J. W., Michel Flores, J., Lavi, A., Abo-Riziq, A., and Rudich, Y.: Changes in the optical properties of benzo[a]pyrene-coated aerosols upon heterogeneous reactions with NO_2 and NO_3, Phys. Chem. Chem. Phys., 13, 6484-6492, doi:10.1039/C0CP02114H, 2011.

Mohr, C., Lopez-Hilfiker, F. D., Zotter, P., Prevot, A. S. H., Xu, L., Ng, N. L., Herndon, S. C., Williams, L. R., Franklin, J. P., Zahniser, M. S., Worsnop, D. R., Knighton, W. B., Aiken, A. C., Gorkowski, K. J., Dubey, M. K., Allan, J. D., and Thornton, J. A.: Contribution of nitrated phenols to wood burning brown carbon light absorption in Detling, United Kingdom during winter time, Environ. Sci. Technol., 47, 6316-6324, doi:10.1021/es400683v, 2013.

Moise, T., Flores, J. M., and Rudich, Y.: Oprtical properties of secondary organic aerosols and their changes by chemical processes, Chem. Rev., 115, 4400-4439, doi:10.1021/cr5005259, 2015.

Mok, J., Krotkov, N. A., Arola, A., Torres, O., Jethva, H., Andrade, M., Labow, G., Eck, T. F., Li, Z., Dickerson, R. R., Stenchikov, G. L., Osipov, S., and Ren, X.: Impacts of brown

carbon from biomass burning on surface UV and ozone photochemistry in the Amazon Basin, Sci. Rep., 6, 36940, doi:10.1038/srep36940, 2016.

Moschos, V., Kumar, N. K., Daellenbach, K. R., Baltensperger, U., Prévôt, A. S. H., and El Haddad, I.: Source Apportionment of Brown Carbon Absorption by Coupling Ultraviolet-Visible Spectroscopy with Aerosol Mass Spectrometry, Environ. Sci. Tech. Let., 5, 302-308, doi:10.1021/acs.estlett.8b00118, 2018.

Nguyen, T. B., Laskin, A., Laskin, J., and Nizkorodov, S. A.: Brown carbon formation from ketoaldehydes of biogenic monoterpenes, Faraday Discuss., 165, 473-494, doi:10.1039/C3FD00036B, 2013.

Ni, H. Y., Huang, R. J., Cao, J. J., Liu, W. G., Zhang, T., Wang, M., Meijer, H. A. J., and Dusek, U.: Source apportionment of carbonaceous aerosols in Xi'an, China: insights from a full year of measurements of radiocarbon and the stable isotope ^{13}C, Atmos. Chem. Phys., 18, 16363-16383, doi:10.5194/acp-18-16363-2018, 2018.

Paatero, P.: Least squares formulation of robust non-negative factor analysis, Chemom. Intell. Lab., 37, 23-35, doi:10.1016/S0169-7439(96)00044-5, 1997.

Park, R. J., Kim, M. J., Jeong, J. I., Yooun, D., and Kim, S.: A contribution of brown carbon aerosol to the aerosol light absorption and its radiative forcing in East Asia, Atmos. Environ., 44, 1414-1421, doi:10.1016/j.atmosenv.2010.01.042, 2010.

Park, S., Yu, G. H., and Lee, S.: Optical absorption characteristics of brown carbon aerosols during the KORUS-AQ campaign at an urban site, Atmos. Res., 203, 16-27, doi:10.1016/j.atmosres.2017.12.002, 2018.

Pillar, E. A., and Guzman, M. I.: Oxidation of substituted catechols at the air-water interface: Production of carboxylic acids, quinones, and polyphenols, Environ. Sci. Technol., 51, 4951- 4959, https://doi.org/10.1021/acs.est.7b00232, 2017.

Ram, K., Sarin, M. M., and Tripathi, S. N.: Temporal trends in atmospheric $PM_{2.5}$, PM_{10}, elemental carbon, organic carbon, water-soluble organic carbon, and optical properties: impact of biomass burning emissions in the Indo-Gangetic Plain, Environ. Sci. Technol., 46, 686-695, doi:10.1021/es202857w, 2012.

Samburova, V., Connolly, J., Gyawali, M., Yatavelli, R. L. N., Watts, A. C., Chakrabarty, R. K.,

Zielinska, B., Moosmüller, H., and Khlystov, A.: Polycyclic aromatic hydrocarbons in biomass-burning emissions and their contribution to light absorption and aerosol toxicity, Sci. Total Environ., 568, 391-401, doi:10.1016/j.scitotenv.2016.06.026, 2016.

Samburova, V., Connolly, J., Gyawali, M., Yatavelli, R. L. N., Watts, A. C., Chakrabarty, R. K., Zielinska, B., Moosmüller, H., and Khlystov, A.: Polycyclic aromatic hydrocarbons in biomass-burning emissions and their contribution to light absorption and aerosol toxicity, Sci. Total Environ., 568, 391-401, doi:10.1016/j.scitotenv.2016.06.026, 2016.

Sengupta, D., Samburova, V., Bhattarai, C., Kirillova, E., Mazzoleni, L., Iaukea-Lum, M., Watts, A., Moosmüller, H., and Khlystov, A.: Light absorption by polar and non-polar aerosol compounds from laboratory biomass combustion, Atmos. Chem. Phys., 18, 10849-10867, doi:10.5194/acp-18-10849-2018, 2018.

Shapiro, E. L., Szprengiel, J., Sareen, N., Jen, C. N., Giordano, M. R., and McNeill, V. F.: Light-absorbing secondary organic material formed by glyoxal in aqueous aerosol mimics, Atmos. Chem. Phys., 9, 2289-2300, doi:10.5194/acp-9-2289-2009, 2009.

Shen, M. L., Xing, J., Ji, Q. P., Li, Z. H., Wang, Y. H., Zhao, H. W., Wang, Q. R., Wang, T., Yu, L. W., Zhang, X. C., Sun, Y. X., Zhang, Z. H., Niu, Y., Wang, H. Q., Chen, W., Dai, Y. F., Su, W. G., and Duan, H. W.: Declining Pulmonary Function in Populations with Long-term Exposure to Polycyclic Aromatic Hydrocarbons-Enriched $PM_{2.5}$, Environ. Sci. Technol., 52, 6610-6616, 2018.

Smith, J. D., Kinney, H., and Anastasio, C.: Phenolic carbonyls undergo rapid aqueous photodegradation to form low-volatility, light-absorbing products, Atmos. Environ., 126, 36-44, doi:10.1016/j.atmosenv.2015.11.035, 2016.

Song, J. Z., Li, M. J., Fan, X. J., Zou, C. L., Zhu, M. B., Jiang, B., Yu, Z. Q., Jia, W. L., Liao, Y. H., and Peng, P. A.: Molecular Characterization of Water- and Methanol-Soluble Organic Compounds Emitted from Residential Coal Combustion Using Ultrahigh-Resolution Electrospray Ionization Fourier Transform Ion Cyclotron Resonance Mass Spectrometry, Environ. Sci. Technol., 53, 13607-13617, doi:10.1021/acs.est.9b04331, 2019.

Srinivas, B., and Sarin, M. M.: Light-absorbing organic aerosols (brown carbon) over the

tropical Indian Ocean: impact of biomass burning emissions, Environ. Res. Lett., 8, 044042, doi:10.1088/1748-9326/8/4/044042, 2013.

Sun, J., Zhi, G., Hitzenberger, R., Chen, Y., Tian, C., Zhang, Y., Feng, Y., Cheng, M., Zhang, Y., Cai, J., Chen, F., Qiu, Y., Jiang, Z., Li, J., Zhang, G., and Mo, Y.: Emission factors and light absorption properties of brown carbon from household coal combustion in China, Atmos. Chem. Phys., 17, 4769-4780, doi:10.5194/acp-17-4769-2017, 2017.

Teich, M., van Pinxteren, D., Kecorius, S., Wang, Z., and Herrmann, H.: First quantification of imidazoles in ambient aerosol particles: potential photosensitizers, brown carbon constituents, and hazardous components, Environ. Sci. Technol., 50, 1166-1173, 2016.

Teich, M., van Pinxteren, D., Wang, M., Kecorius, S., Wang, Z., Müller, T., Mocnik, G., and Herrmann, H.: Contributions of nitrated aromatic compounds to the light absorption of water-soluble and particulate brown carbon in different atmospheric environments in Germany and China, Atmos. Chem. Phys., 17, 1653-1672, doi:10.5194/acp-17-1653-2017, 2017.

Wang, G. H., Kawamura, K., Lee, S., Ho, K. F., and Cao, J. J.: Molecular, seasonal, and spatial distributions of organic aerosols from fourteen Chinese cities, Environ. Sci. Technol., 40, 4619-4625, doi:10.1021/es060291x, 2006.

Wang, J. Z., Ho, S. S. H., Huang, R. J., Gao, M. L., Liu, S. X., Zhao, S. Y., Cao, J. J., Wang, G. H., Shen, Z. X., and Han, Y. M.: Characterization of parent and oxygenated-polycyclic aromatic hydrocarbons (PAHs) in Xi'an, China during heating period: An investigation of spatial distribution and transformation, Chemosphere, 159, 367-377, doi:10.1016/j.chemosphere.2016.06.033, 2016.

Wang, L. W., Wang, X. F., Gu, R. R., Wang, H., Yao, L., Wen, L., Zhu, F. P., Wang, W. H., Xue, L. K., Yang, L. X., Lu, K. D., Chen, J. M., Wang, T., Zhang, Y. H., and Wang, W. X.: Observations of fine particulate nitrated phenols in four sites in northern China: concentrations, source apportionment, and secondary formation, Atmos. Chem. Phys., 18, 4349-4359, doi:10.5194/acp-18-4349-2018, 2018.

Washenfelder, R. A., Attwood, A. R., Brock, C. A., Guo, H., Xu, L., Weber, R. J., Ng, N. L., Allen, H. M., Ayres, B. R., Baumann, K., Cohen, R. C., Draper, D. C., Duffey, K. C.,

685 Edgerton, E., Fry, J. L., Hu, W. W., Jimenez, J. L., Palm, B. B., Romer, P., Stone, E. A.,
686 Wooldridge, P. J., and Brown, S. S.: Biomass burning dominates brown carbon absorption
687 in the rural southeastern United States, Geophys. Res. Lett., doi:10.1002/2014GL062444,
688 42, 653-664, 2015.
689 Xie, M. J., Chen, X., Hays, M. D., Lewandowski, M., Offenberg, J., Kleindienst, T. E., and
690 Holder, A. L.: Light absorption of secondary organic aerosol: composition and
691 contribution of nitroaromatic compounds, Environ. Sci. Technol., 51, 11607-11616,
692 doi:10.1021/acs.est.7b03263, 2017.
693 Xie, M. J., Chen, X., Holder, A. L., Hays, M. D., Lewandowski, M., Offenberg, J. H.,
694 Kleindienst, T. E., Jaoui, M., and Hannigan, M. P.: Light absorption of organic carbon and
695 its sources at a southeastern U.S. location in summer, Environ. Pollut., 244, 38-46,
696 doi:10.1016/j.envpol.2018.09.125, 2019.
697 Yan, C. Q., Zheng, M., Sullivan, A. P., Bosch, C., Desyaterik, Y., Andersson, A., Li, X. Y., Guo,
698 X. S., Zhou, T., Gustafsson, O., and Collett Jr, J. L.: Chemical characteristics and light-
699 absorbing property of water-soluble organic carbon in Beijing: Biomass burning
700 contributions, Atmos. Environ., 121, 4-12, doi:10.1016/j.atmosenv.2015.05.005, 2015.
701 Yan, C. Q., Zheng, M., Bosch, C., Andersson, A., Desyaterik, Y., Sullivan, A. P., Collett, J. L.,
702 Zhao, B., Wang, S. X., He, K. B., and Gustafsson, Ö.: Important fossil source contribution
703 to brown carbon in Beijing during winter, Sci. Rep., 7, 43182, doi:10.1038/srep43182,
704 2017.
705 Zhang, X., Lin, Y.-H., Surratt, J. D., and Weber, R.: Sources, composition and absorption
706 Ångström exponent of light-absorbing organic components in aerosol extracts from the
707 Los Angeles Basin, Environ. Sci. Technol., 47, 3685-3693, doi:10.1021/es305047b, 2013.
708 Zhang, Y., Forrister, H., Liu, J., Dibb, J., Anderson, B., Schwarz, J. P., Perring, A. E., Jimenez,
709 J. L., Campuzano-Jost, P., Wang, Y., Nenes, A., and Weber, R. J.: Top-of-atmosphere
710 radiative forcing affected by brown carbon in the upper troposphere, Nat. Geosci., 10, 486-
711 489, doi:10.1038/NGEO2960, 2017a.
712 Zhang, Y., Xu, J., Shi, J., Xie, C., Ge, X., Wang, J., Kang, S., and Zhang, Q.: Light absorption
713 by water-soluble organic carbon in atmospheric fine particles in the central Tibetan Plateau,

714 Environ. Sci. Pollut. Res., 24, 21386–21397, doi:10.1007/s11356-017-9688-8, 2017b.
715 Zhong, M., and Jang, M.: Dynamic light absorption of biomass-burning organic carbon
716 photochemically aged under natural sunlight, Atmos. Chem. Phys., 14, 1517-1525, 2014.
717 Zhu, C. S., Cao, J. J., Huang, R. J., Shen, Z. X., Wang, Q. Y., and Zhang, N. N.: Light absorption
718 properties of brown carbon over the southeastern Tibetan Plateau, Sci. Total Environ., 625,
719 246-251, doi:10.1016/j.scitotenv.2017.12.183, 2018.

720 **Table 1.** Annual and seasonal mean contributions of measured PAHs, NACs and MOPs to
721 methanol-soluble BrC light absorption at 365 nm. Hyphens denote the measured value of more
722 than one third of the samples is below the detection limit.

Compounds	MAE_{365}	Contribution to BrC light absorption at 365 nm (%)				
	(m^2 gC^{-1})	Annual	Spring	Summer	Fall	Winter
Fluoranthene (FLU)	4.25	0.11	0.05	0.02	0.05	0.15
Pyrene (PYR)	0.46	0.01	0.00	0.00	0.01	0.01
Chrysene (CHR)	0.00	0.00	0.00	0.00	0.00	0.00
Benzo(a)anthracene (BaA)	2.06	0.04	0.01	0.01	0.02	0.05
Benzo(a)pyrene (BaP)	9.31	1.04	0.76	0.39	1.16	1.10
Benzo(b)fluoranthene (BbF)	4.10	0.17	0.14	0.07	0.17	0.18
Benzo(k)fluoranthene (BkF)	3.47	0.04	0.03	0.02	0.04	0.04
Indeno[1,2,3-cd]pyrene (IcdP)	4.68	0.51	0.50	0.24	0.71	0.46
Benzo(ghi)perylene (BghiP)	8.95	0.29	0.28	0.16	0.41	0.26
9,10-Anthracenequinone (9,10AQ)	0.28	0.01	0.00	0.00	0.00	0.01
Benzanthrone (BEN)	6.13	0.11	0.08	0.05	0.11	0.12
Benzo[b]fluoren-11-one (BbF11O)	1.89	0.02	0.02	0.01	0.02	0.03
4-Nitrophenol (4NP)	2.17	0.08	0.06	0.02	0.05	0.10
4-Nitro-1-naphthol (4N1N)	9.71	-	-	-	-	0.03
2-Methyl-4-nitrophenol (2M4NP)	2.81	0.03	0.01	0.01	0.01	0.04
3-Methyl-4-nitrophenol (3M4NP)	2.65	0.02	0.01	0.00	0.01	0.03
2,6-Dimethyl-4-nitrophenol (2,6DM4NP)	3.27	-	-	-	-	0.01
4-Nitrocatechol (4NC)	7.91	0.27	0.05	0.03	0.20	0.35
3-Methyl-5-nitrocatechol (3M5NC)	5.77	-	-	-	0.05	0.11
4-Methyl-5-nitrocatechol (4M5NC)	7.29	-	-	-	0.06	0.13
3-Nitrosalicylicacid (3NSA)	3.86	-	-	-	-	0.01
5-Nitrosalicylicacid (5NSA)	3.36	0.03	0.01	0.02	0.04	0.02
Syringyl acetone (SyA)	0.25	0.01	0.01	0.00	0.01	0.01
Vanillin (VAN)	8.17	0.01	0.00	0.00	0.00	0.01
Vanillic acid (VaA)	0.66	0.00	0.00	0.00	0.00	0.00
Total	103.46	2.80	2.02	1.05	3.13	3.26

723 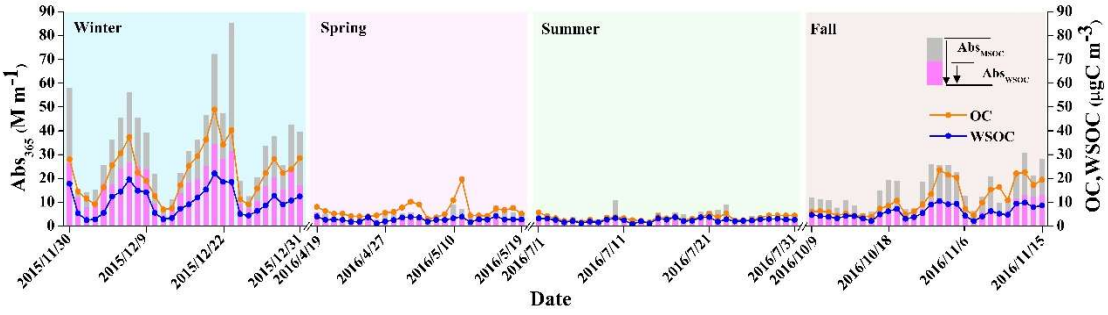

724 **Figure 1.** Time series of the light absorption coefficient of water-soluble and methanol-soluble
725 BrC at 365 nm ($Abs_{365,WSOC}$ and $Abs_{365,\ MSOC}$, respectively), as well as OC and WSOC
726 concentrations.

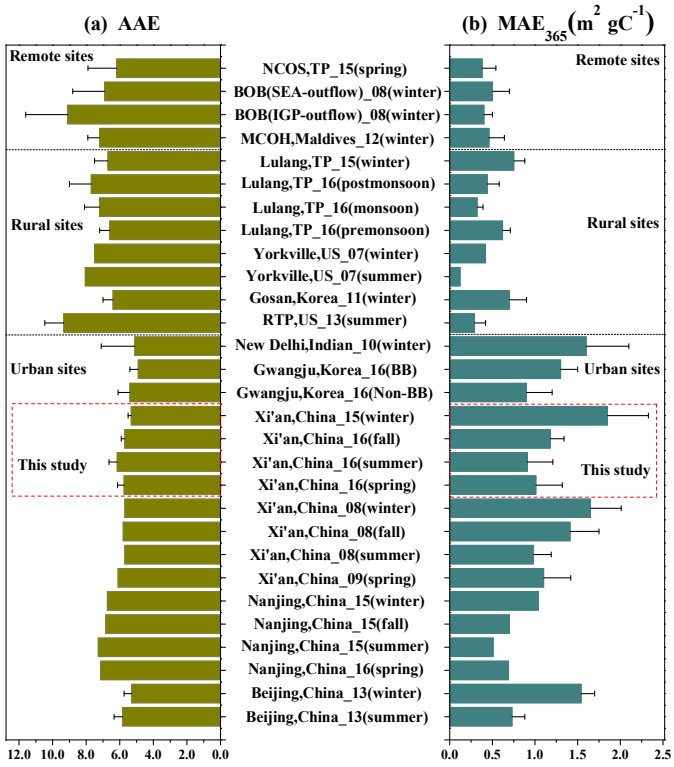

Figure 2. Comparison of AAE (left column) and MAE_{365} (right column) values of water-soluble BrC at remote sites (Srinivas and Sarin, 2013; Bosch et al., 2014; Zhang et al., 2017b), rural sites (Hocobian et al., 2010; Kirillova et al., 2014a; Zhu et al., 2018; Xie et al., 2019) and urban sites (Kirillova et al., 2014b; Yan et al., 2015; Chen et al., 2018; Huang et al., 2018; Park et al., 2018).

733

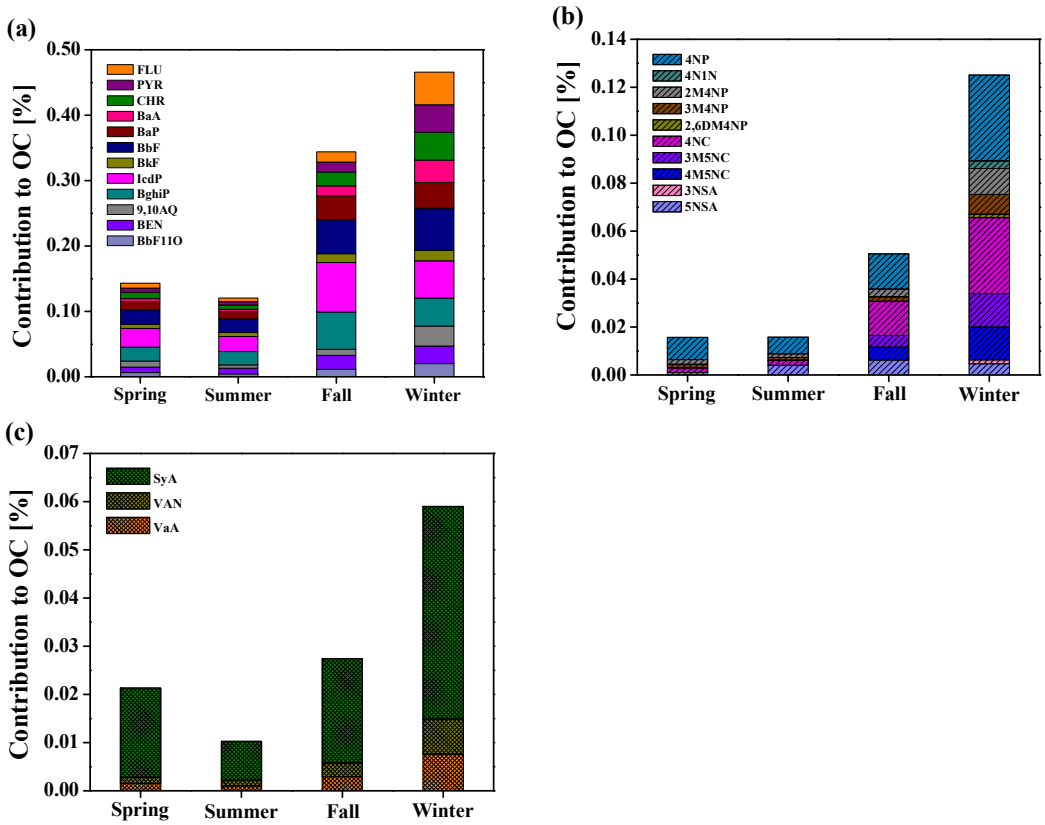

734
735

736 **Figure 3.** Contributions of (a) PAHs, (b) NACs, and (c) MOPs carbon mass concentrations to

737 the total OC concentrations.

738

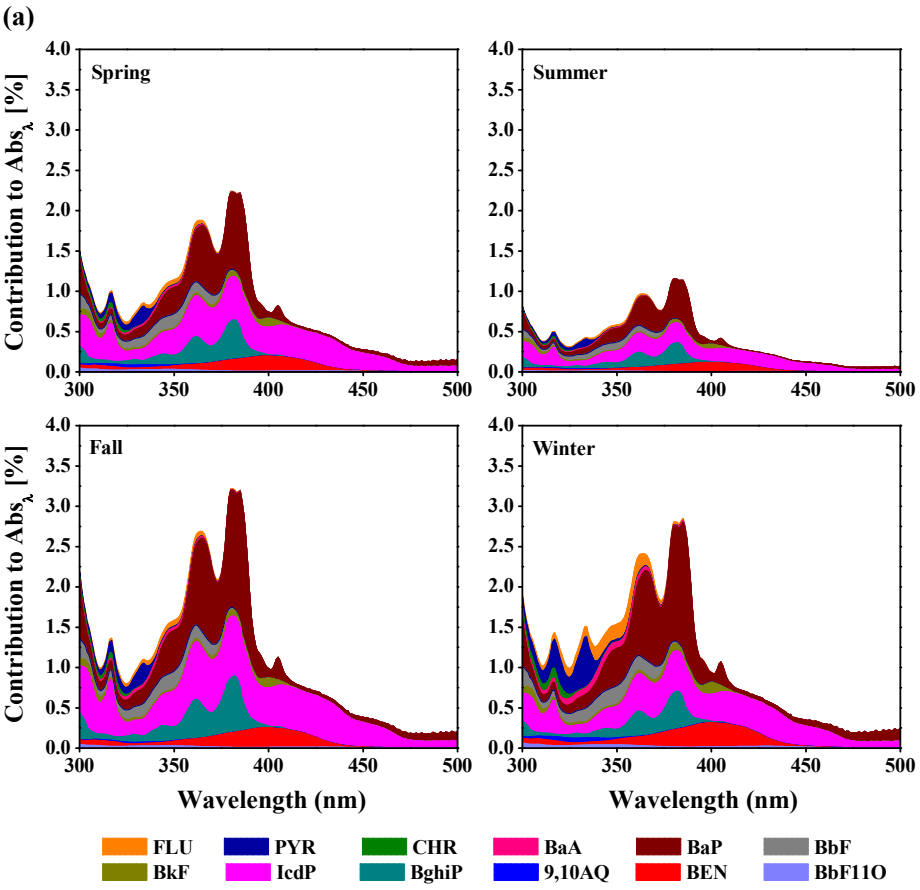
(a)
Spring
Summer
Fall
Winter
Contribution to Abs$_\lambda$ [%]
Wavelength (nm)
FLU
PYR
CHR
BaA
BaP
BbF
BkF
IcdP
BghiP
9,10AQ
BEN
BbF11O

739

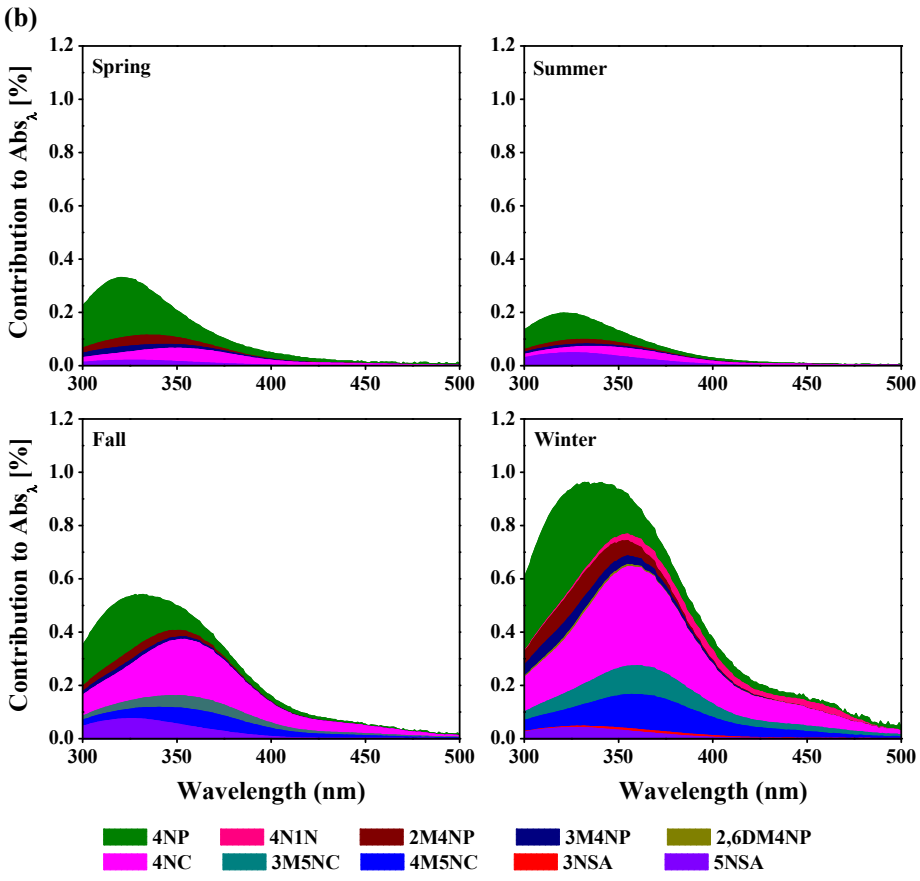
(b)
Spring
Summer
Fall
Winter
Contribution to Abs$_\lambda$ [%]
Wavelength (nm)
4NP
4N1N
2M4NP
3M4NP
2,6DM4NP
4NC
3M5NC
4M5NC
3NSA
5NSA

740

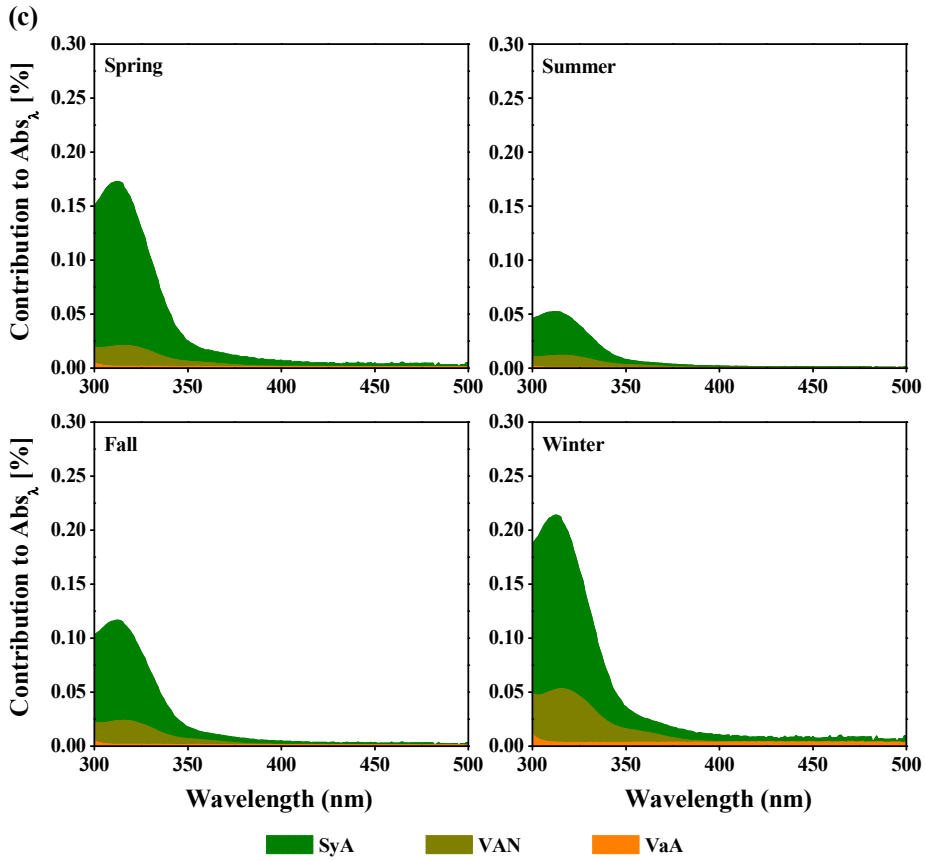

741

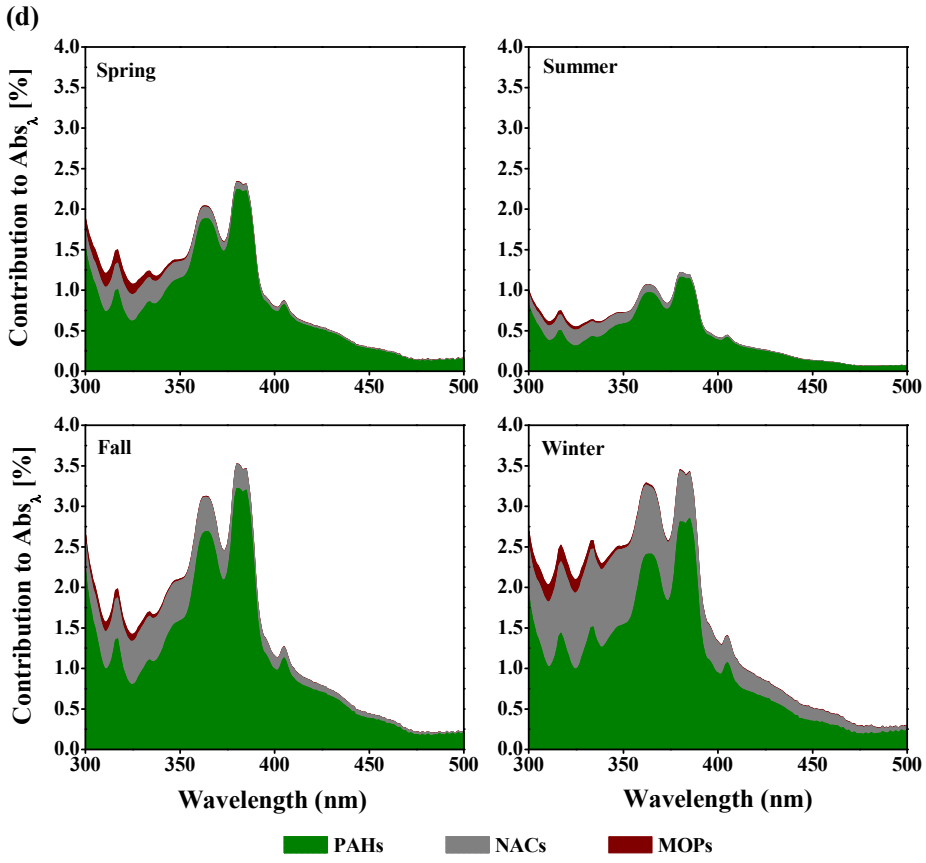

742

743 **Figure 4.** Light absorption contributions of (a) PAHs, (b) NACs, (c) MOPs and (d) total

744 measured chromophores to Abs_{MSOC} over the wavelength range of 300 to 500 nm in spring,
745 summer, fall and winter.
746

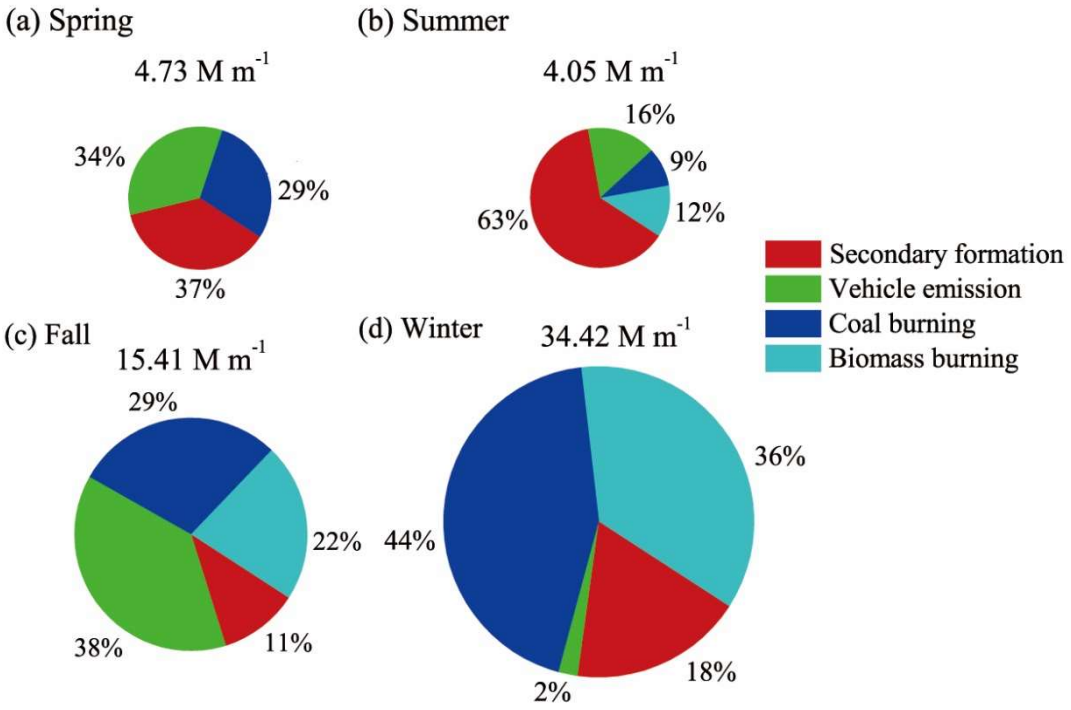

747

748 **Figure 5.** Contributions of the major sources to $Abs_{365,MSOC}$ in Xi'an during spring, summer, fall

749 and winter.